ACS APPLIED MATERIALS & INTERFACES

Research Article

www.acsami.org

Mixed Phytochemicals Mediated Synthesis of Multifunctional Ag–Au–Pd Nanoparticles for Glucose Oxidation and Antimicrobial Applications

K. Jagajjanani Rao and Santanu Paria*

Interfaces and Nanomaterials Laboratory, Department of Chemical Engineering, National Institute of Technology, Rourkela-769 008, Orissa India

Supporting Information

ABSTRACT: The growing awareness toward the environment is increasing commercial demand for nanoparticles by green route syntheses. In this study, alloy-like Ag–Au–Pd trimetallic nanoparticles have been prepared by two plants extracts *Aegle marmelos* leaf (LE) and *Syzygium aromaticum* bud extracts (CE). Compositionally different Ag–Au–Pd nanoparticles with an atomic ratio of 5.26:2.16:1.0 (by LE) and 11.36:13.14:1.0 (by LE + CE) of Ag:Au:Pd were easily synthesized within 10 min at ambient conditions by changing the composition of phytochemicals. The average diameters of the nanoparticles by LE and LE + CE are ∼8 and ∼11 nm. The catalytic activity of the trimetallic nanoparticles was studied, and they were found to be efficient catalysts for the glucose oxidation process. The prepared nanoparticles also exhibited efficient antibacterial activity against a model Gram-negative bacteria *Escherichia coli*. The catalytic and antimicrobial properties of these readymade trimetallic nanoparticles have high possibility to be utilized in diverse fields of applications such as health care to environmental.

KEYWORDS: *green synthesis, Aegle marmelos, Syzygium aromaticum, alloy-like, catalysts, antimicrobial*

1. INTRODUCTION

The bimetallic and trimetallic nanoparticles (NPs) are of increasing interest in recent years because of their novel properties and applications.[1−3] The preparation of multimetallic NPs usually involves the formation of an alloy or core/shell type structures, and they possess improved physicochemical properties in comparison to their monometallic counterparts.[4] Among multimetallic NPs, bimetallic and trimetallic NPs have scientific and industrial importance because of their novel properties namely, magnetic, optical, electronic, and catalytic for practical applications.[1,4] Bimetallic NPs were conventionally produced by seed-mediated growth, template synthesis, chemical reduction, and laser ablation, etc.[4] Moreover, reported studies showed well dispersed trimetallic NPs usually synthesized by colloidal chemical[5] methods with additives like surfactants or stabilizers,[2,3,6] chemically designed self-organization reaction,[7] laser-induced alloying,[8] thermal heating,[9] and so on. Coming to catalytic property in glucose oxidation reactions, in particular, trimetallic NPs exhibit higher potential than the bimetallic and monometallic ones.[10,11] The Au NPs have been proved to be effective catalysts for the selective oxidation of glucose to gluconates in competition with enzymatic catalysis and have the advantage to work in a wide range of pH, from alkaline to acidic conditions.[12] Numerous studies addressed the catalytic ability of mono and bimetallic Au NPs for glucose oxidation and Au containing trimetallic NPs, in the form of alloy, or core–shell structures are under the focus.[5,7,8,12] Similar to bimetallic NPs, the synthesis of trimetallic NPs was also favored by widespread chemical methods.[5,8,10,11] However, the utilization of costly and toxic chemicals, multistep procedures, the requirement of specialized and expensive equipment pose major hurdles for the large scale synthesis of novel trimetallic NPs.

The growing concerns toward the green technology necessitate the development of new and eco-friendly techniques for the synthesis of different NPs. During the past decade, a series of distinct methods have been reported to synthesize various size/shape NPs by bio and nonbiological green approaches.[13,14] Among biogenic approaches, NPs synthesis by the help of phytochemicals is intensely attracting researchers attention because of their inherent advantages like simple, nontoxic, eco-friendly etc.,.[4,13,14] Aiming at cost effectiveness and process simplicity, significant attempts on the biosynthesis of bimetallic NPs were already reported on Au containing Ag–Au NPs using various plant bioresources.[15,16] While considering the trimetallic NPs, Au–Pt–Ag[17] and Au–Pd–Pt[9,18] were

Received: April 12, 2015
Accepted: June 4, 2015
Published: June 4, 2015

DOI: 10.1021/acsami.5b03089
ACS Appl. Mater. Interfaces 2015, 7, 14018−14025

synthesized by microwave mediated method (the only reported greener approach). To the best of our knowledge, there is only one study reported for the synthesis of trimetallic NPs by plant resources which is an *in vivo* approach.[19] The mentioned study showed the production of Au−Ag−Cu alloy type NPs (5−50 nm) by *Brassica juncea*.

In this study, we report a simple, efficient, reproducible, and green method for the synthesis of well-dispersed trimetallic Ag−Au−Pd alloy NPs using plant resources (*A. marmelos leaf* and *Syzygium aromaticum* bud extracts) and a natural surfactant (*Acacia auriculiformis*). The synthesis involves synchronized addition of respective metal precursors in aqueous media by following a single step approach. Preparation, characterization, and spectral properties of the prepared particles are presented and discussed.

From the application perspective, among several applications Au-based NPs are important toward glucose oxidation.[5,12,20] In general, catalysts are expected to be active either in the form of supports on other material or particles suspension, and should be having working ability in a wide range of pH (alkaline to acidic conditions).[20] The prepared trimetallic NPs have been utilized as catalysts for glucose oxidation to obtain gluconic acid under mild conditions. The NPs with Au−Ag−Pd in this study have the advantage of the elimination of catalyst deactivation and side reactions (which are usually seen in reactions with Bi−Pd and Bi−Pd−Pt NPs).[20] Additionally, the presence of Ag avoids contamination of the reaction media particularly biochemicals (e.g., glucose).[20] Facile green synthesis of smaller size Ag−Au−Pd alloy NPs using plant extracts in this study is first of its kind and this study showed the use of renewable resources for clean synthesis of trimetallic NPs unlike the reported studies.[2,3,5−8,10,11] Owing to its catalytic activity, it has huge scope toward commercialization viewpoint. Previously reported trimetallic NPs are mainly Pt-based, which are expensive than that of Pd-based, used in this study.[17,18] Furthermore, in support to our claim the antimicrobial activity of the NPs were evaluated against a model Gram-negative bacterium *Escherichia coli* and achieved promising results. The performed applications of the as-prepared NPs have huge scope as multifunctional agent such as industrial catalysts with the effective antimicrobial property.

2. EXPERIMENTAL SECTION

2.1. Materials and Methods. The chloroauric acid ($HAuCl_4$) was purchased from Loba Chemie, India. Silver nitrate ($AgNO_3$), sodium chloride (NaCl), sodium hydrogen carbonate ($NaHCO_3$), sodium gluconate from Merck, India. Palladium chloride ($PdCl_2$) was purchased from Sigma-Aldrich. Here, 1 M $PdCl_2$ was solubilized in the presence of 2 M NaCl to form 1 M Na2$PdCl_4$ prior to experimentation. The ultrapure water of 18.2 mΩ.cm resistivity was used throughout the study. *Aegle marmelos* leaf extract (LE) was prepared according to our previous study.[21] The extractions of plant surfactant *A. auriculiformis*[22] and clove bud (CE)[23] were prepared as per our previously reported methods. A 5% stock solution of LE and clove bud extract (CE) was prepared in deionized water from the freeze-dried powder and used for the experimentations.

2.2. Preparation Ag−Au−Pd Trimetallic Nanoparticles. The method involves simultaneous reduction of metal precursors ($AgNO_3$, $HAuCl_4$, and Na_2PdCl_4) under optimum controlled conditions. The optimum conditions used in the study were established in our previous study[24] to have possible smaller size monometallic Ag NPs of ∼13 nm. The initial synthesis conditions are pH (7.0), additive (Acacia 0.428 mM), temperature (55 °C), metal salt/plant extract ratio (1 mM/0.3%) at normal daylight conditions for the production of trimetallic Ag−Au−Pd alloy NPs. The synthesis step involves the addition of $AgNO_3$ first and after 30 s, other two metal salts Au and Pd were added immediately one after another in aqueous media. Here the addition of Ag salt at first avoids the chance of AgCl precipitation during the reaction as the other two precursors are in chloride form. The formation of NPs is very quick, and visible color changes were observed instantaneously. After 10 min of equilibration, the NPs were collected via centrifugation and subjected to further analysis. The strength of metal salts used in the study was 1 mM each.

The LE in the stated procedure was partly and fully replaced with the same strength of CE in various proportions (1:0, 1:1 and 0:1) to produce various sizes and proportionally different Ag−Au−Pd trimetallic NPs.

2.3. Glucose Oxidation by Ag−Au−Pd NPs. The average molar mass of the respective NPs were calculated from the mass fractions (from TEM-EDX analysis) of the proportionally different trimetallic NPs produced (detail given in Supporting Information, SI−I). The molar mass identified to be 130 g/mol for LE produced trimetallic NPs, while it is 140 g/mol for LE+CE produced trimetallic NPs. These values are considered, and the performances of individual trimetallic NPs were evaluated by glucose oxidation as a model reaction. The procedure stated by Comotti et al.[20] was slightly modified for the oxidation process. Glucose used in the study was 400 mM. Initially, glucose and catalyst (glucose: total metal = 3000) in deionized water were stirred (at 1500 rpm using a magnetic stirrer) in a temperature controlled glass reactor vessel. The reactions were carried out at 60 °C with initial pH of ∼9.5 for 190 min. The temperature during the experimentations was maintained and controlled by IKA RCT basic hot plate stirrer, equipped with a temperature probe. The mean value of the measured catalytic activities was used as the turn over frequency [TOF] value (mol glucose/total moles of metal/h).

Glucose oxidation was quantitatively monitored by the estimation of produced gluconic acid using aluminum salt solution.[25] The method in brief is as follows: the presence of $Al(SO_4)(H_2O)_5^+$ would reduce the amount of hydroxide form of Al for absorption in aqueous medium devoid of any complexing agent like gluconic acid. Here gluconic acid loosens sulfate interaction with the inner-coordination sphere of Al(III) in $Al(SO_4)(H_2O)_5^+$ and increases the UV absorption (linearly at 240 nm) of aluminum salt solution by forming $Al(OH)(H_2O)_5^{2+}$. The calibration curve was plotted using standard sodium gluconate with aluminum salt solution (of ∼pH 4) for quantitative estimation. Thus, the depletion of glucose was measured by the generation of gluconic acid in the reaction medium after the end incubation time of 190 min.

2.4. Bacterial Sensitivity Tests. The synthesized two proportionally different Ag−Au−Pd NPs (∼8 and ∼11 nm) were tested for the antibacterial activity by well-diffusion method against *Escherichia coli* (NCIM 5051) bacteria. The pure culture of the organism was subcultured and maintained on nutrient agar (NA) prior to the study. In this study, 20 μL from 0.1 mM of respective trimetallic NPs with different proportions were added into 4 mm wells of *E. coli* amended agar plates. A 2% w/v *E. coli* culture was used for the study and agar wells were made on NA plates using a sterile cork borer. After incubating plates at 37 °C for 48 h, different levels of zone of inhibition (ZOI) were measured as follows:

ZOI (mm) = total diameter of the clear zone−diameter of the agar well. Reaction media devoid of metal salts served as controls. The diameter of the inhibition zone was measured at a 90° angle using Digisoft ProMed software, and the measurements were averaged. Morphological changes in the used microorganisms after exposure to respective NPs in aqueous media were observed by SEM/FSEM analysis wherever necessary

2.5. Characterization. UV−visible spectra of trimetallic NPs were recorded using a UV−visible-NIR spectrophotometer (Shimadzu, UV-3600). High-resolution transmission electron microscopy (HRTEM, JEOL-2100F) and field emission scanning electron microscopy (NOVA-NANO SEM 450) were used to identify the particle sizes and shapes wherever necessary. Participation of the active functional groups was identified by FT-IR (Thermo Fisher, Nicolet iS10) operated in attenuated total reflectance (ATR) mode with zinc selenide (ZnSe) crystal. The powder X - ray diffraction measurements

DOI: 10.1021/acsami.5b03089
ACS Appl. Mater. Interfaces 2015, 7, 14018−14025

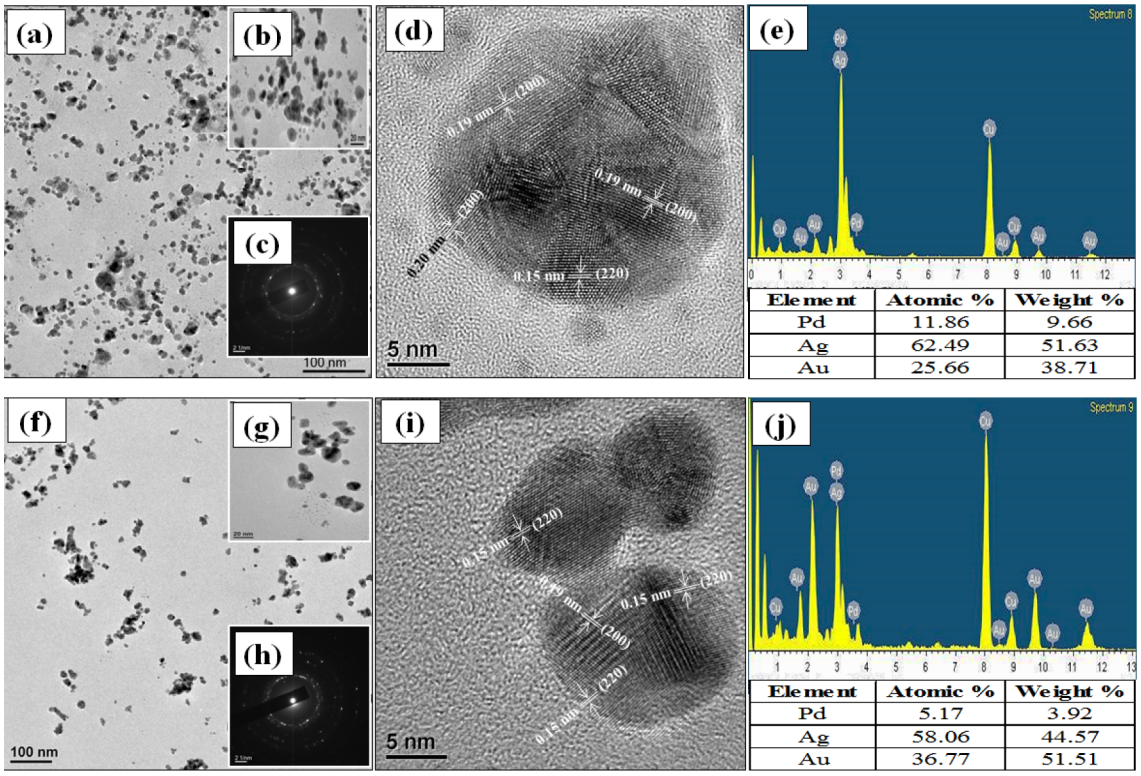

Figure 1. TEM analysis of Ag−Au−Pd NPs prepared by LE (a−e) and LE + CE (f−j) extracts in aqueous media. Low magnification (a, f), high magnification (b, g), SAED (c, h), fringe pattern (d, i) along with EDX (e, j) was shown.

were performed by Philips (PW1830 HT) X-ray diffractometer at 0.05°/s with an accelerating voltage of 35 kV and with an applied current of 30 mA.

3. RESULTS AND DISCUSSION

3.1. Microscopic Analysis of the Trimetallic Nanoparticles. Multimetallic NPs are generally synthesized in the solution media by successive reduction of respective precursors.[3] Mostly in this process one of the metal salts is reduced first and then the second metal is deposited to form a core/shell, composite, or alloy type NPs. In our study, primarily $AgNO_3$ was added first among the used metal ion precursors (as stated in section 2.2) to attain trimetallic NPs. The trimetallic NPs from LE + CE of proportion 1:0 were analyzed using TEM as shown in Figure 1a−e. The formed particles are near spherical in shape (Figure 1a and b), and the average particle size is ∼8.16 ± 4.2 nm, obtained from the histogram (Figure S1a, Supporting Information). Figure 1c shows the selected area electron diffraction (SAED) pattern obtained from a selected area of Figure 1b. The bright rings with occasional bright spots are because of the presence of polycrystals.[3] The ring pattern indexing of Figure 1c (detailed in Figure S2a, Supporting Information) displayed d-values of 2.20, 1.98, 1.36, and 1.12 Å, correspond to (111), (200), (220), and (311) planes respectively of face-centered cubic (fcc) structure, which are intermediate values between their pure Ag, Au, and Pd NPs (JCPDS Nos. 04-0783, 04-0784, 87-0638 respectively) and the values are near to the lattice planes of Pd NPs (2.236, 1.936, 1.369, 1.170). In addition to the above, the calculated d-values from the lattice fringe pattern (from Figure 1d) are 0.15 and 0.19 nm correspond to Ag and Au with lattice planes (220), (200) respectively, and the *d*-values of 0.193 and 0.196 nm corresponds to the presence of lattice planes (200), (200) of Pd in the trimetallic Au−Ag−Pd NPs. The EDX analysis of imaged particles was performed to assess the changes in particle composition (Figure 1e). The compositional atomic ratio of 5.26:2.16:1.0 (Ag:Au:Pd) obtained from the LE-assisted synthesized trimetallic NPs, is different than the used stoichiometric ratio.

Furthermore, trimetallic NPs were also synthesized by 1:1 ratio of LE and CE (indicated as LE + CE) and the TEM analysis is shown in Figure 1f. Figure 1f shows the size and homogeneity of the Au−Ag−Pd trimetallic NPs formed from LE + CE extract. The closer view of the NPs is shown in Figure 1g and the average size of the particles were found to be ∼11.61 ± 6.5 nm (Figure S1b, Supporting Information). The SAED pattern (Figure 1h) shows the d- values are 2.30, 1.96, 1.36, and 1.16 Å (Figure S2b, Supporting Information), which are very near to Ag and Au NPs (JCPDS Nos. 04-0783, 04-0784) and correspond to (111), (200), (220), and (311) planes of fcc structure. A close view of NPs displayed the fringe patterns (Figure 1i), and the distances of the lattice fringes are measured at various portions of the imaged particles. The *d*-values of 0.15 nm corresponds to (220) lattice plane Ag or Au elements in the particles, whereas 0.19 nm is due to (200) lattice plane of element Pd. Furthermore, EDX analysis in conjunction with TEM reveals the localized elemental composition as shown in Figure 1j. The formed trimetallic NPs show a compositional atomic ratio of 11.36:13.14:1.0 (Ag/Au/Pd), indicate the low Pd content in the trimetallic NPs compared to that of only LE. The compositional differences of the NPs obtained from two methods lead to the difference in the d-values calculated from the ring patterns. The *d*-values of the lattice planes deviate from Ag or Au crystalline profile toward Pd when Pd loading is more (Figure S2, Supporting Information). This study indicates the

DOI: 10.1021/acsami.5b03089
ACS Appl. Mater. Interfaces 2015, 7, 14018−14025

use of mixed phytochemicals can vary the composition of the trimetallic nanoparticle.

The literature suggests, metallic NPs, especially noble metals, give high contrast in the TEM imaging.[26] The high contrast regions in Figures 1d and i can be attributed to the presence of noble elements (Au and Ag) in the formed NPs. The characteristic alloy type feature is also clearly evident from trimetallic NPs obtained from LE and LE + CE as there is no clear differentiation of phase structure in the imaged particles (Figures 1 and S3, Supporting Information). Also, irregular contrast and lattice planes crossovers in the TEM images further support our assumption. In this study, Au and Pd precursors were added in the presence of green reducing agents onto preformed Ag seeds. May be there was a possibility for core/shell morphology. However, the TEM images suggest the formation of alloy type NPs. Alloy type NPs are formed because of simultaneous reduction of metal precursors. Needless to say, there might be a chance of partial galvanic replacement reaction too, which is also helping the formation of alloy type NPs. Galvanic replacement reaction occurs spontaneously when atoms of a metal (zero valence state) reacts with ions of another metal having a higher electrochemical potential in a solution phase. The reduction process occurs in the absence of the external reducing agent. Generally, in galvanic replacement process lower standard electrode potential metal is used as a sacrificial layer. In our case, standard reduction potentials of Ag, Pd, and Au are +0.80, +0.95, and +1.50 V respectively. Since plant extracts act as reducing agent, chances of galvanic reaction are less but still possible. We believe that when Au and Pd precursors are added; they were reduced by the plant extracts and at the same time, Ag also comes out because of galvanic replacement and mixed in the Au, Pd layer to form a better alloy type structure.

Additionally, trimetallic NPs from only CE was also analyzed by FE-SEM and shown in Figure S4, Supporting Information. Unlike other two cases, larger size particles (~20 and 200 nm, Figure S4b, Supporting Information) with higher polydispersity were obtained in this case (Figure S4a, Supporting Information). The apparent occurrence of larger size particles was already reported for Au NPs using CE.[23] The reported study stated that rapid synthesis within few minutes is key step in obtaining irregular size/shape NPs of sizes 5−100 nm. We assume the similar behavior is responsible in attainment of larger size trimetallic NPs by CE in this study also. Mapping analysis revealed that the trimetallic particles are composed of Ag−Au−Pd with low Pd loading (Figure S4c, Supporting Information). Since our intention here is to have smaller, and uniform size particles, NPs from only CE are not considered for further experimentation.

3.2. UV−Visible Analysis. The UV−vis spectra of the Ag−Au−Pd NPs from LE and LE + CE are shown in Figure 2. The color changes after reduction, because of the formation of particles are given in Figure 2 insets and can be attributed to the size dependent surface plasmon resonance (SPR) effect. The NPs suspensions from LE and LE + CE displayed absorption spectra with single peaks with maximum absorptions at 458 and 550 nm, respectively. Upon comparison with EDX analysis of NPs (Figure 1), it is remarkable to note that the shift in absorption band toward red region in the case of LE + CE mediated NPs because of more Au content. In addition to the above, the shape of absorbance spectra with single plasmonic band infer the nature of alloy type NPs[27] and support the morphologies obtained by HR-TEM analysis.

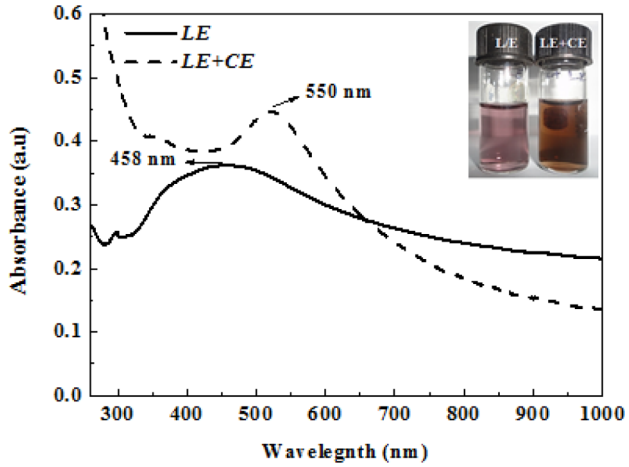

Figure 2. UV−visible spectra of Au−Ag−Pd NPs formed from LE and LE + CE. Figure inset shows the color change because of trimetallic NPs formation in LE and LE + CE systems. Here LE is *A. marmelos* leaf extract and CE represents *S. aromaticum* bud extract.

3.3. XRD Analysis. To elucidate the phase changes in detail, XRD patterns of the trimetallic NPs were investigated and shown in Figure 3. The broad bands in the XRD profile of the as-synthesized trimetallic NPs are indicative of the formation of fine particles.[8,28] The peak maximum (38.27° for LE, 38.26° for LE+C) of these broad bands was located in between the (111) reflections of the pure Pd and Au or Ag NPs. This suggests the formation of alloy-like trimetallic NPs by LE and LE+CE.[8] Furthermore, by comparing the diffractograms of two trimetallic NPs (Figure 3), we can observe a noteworthy change in the intensity at 2θ values from ~35 to 50°. The % crystallinity values are 31.53 and 16.07% for trimetallic NPs obtained from LE+CE and LE (Supporting Information, SI−II). These values indicate that the crystallinity decreases with increase in Pd loading of the trimetallic NPs. Furthermore, using Scherrer equation the crystallite size of trimetallic NPs is calculated from XRD data. The calculated average crystallite sizes of particles obtained from LE and LE+CE are 11.16 and 10.45 nm, respectively. The obtained sizes are very near to the calculated sizes obtained from TEM analysis, which is noteworthy.

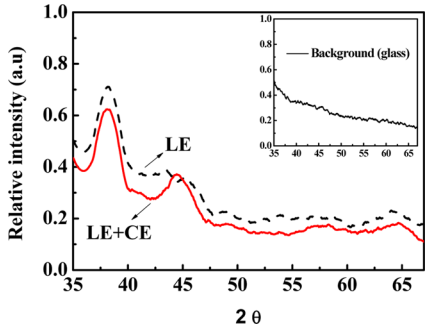

Figure 3. XRD patterns of the Au−Ag−Pd NPs formed from LE and LE + CE. Figure inset shows the background spectra (glass) used for the analysis.

3.4. FT-IR Analysis. Tannins of LE and flavonoids of CE play dual roles in this process by reducing the metal precursors and stabilizing the formed NPs.[21,23] The FT-IR spectra of water washed trimetallic NPs from LE and LE + CE shows significant

DOI: 10.1021/acsami.5b03089
ACS Appl. Mater. Interfaces 2015, 7, 14018−14025

absorption bands indicated in Figure 4 and Table S1, Supporting Information. The spectral bands of trimetallic

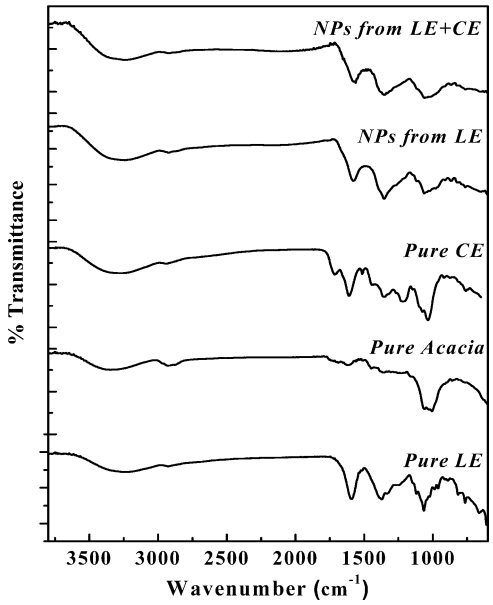

Figure 4. FTIR spectra of the various plant resources used in the study to attain Au–Ag–Pd NPs from LE and LE + CE. The representations are as follows: LE, *A. marmelos* leaf extract; CE, *S.aromaticum* bud extract; acacia, *A. auriculiformis*.

NPs from LE are very close to the polyphenols of LE which infers to the capping effect of plant extract (Table S1, Supporting Information) and the trimetallic NPs from LE + CE showed the presence of mixed functional groups from LE and CE (Table S1, Supporting Information). Most importantly, the presence of geminal methyl groups of CE and major peaks of LE confirm the cumulative effect of both extracts in stabilizing the NPs.

3.5. Glucose Oxidation Study. Gluconic acid from glucose or glucose-containing raw materials is an industrially significant product in the fields of food and pharmaceuticals industries, widely used as water-soluble cleansing agents or additives for food and beverages.[11,20] Industrially it is produced by enzymatic oxidation of D-glucose using molds.[20] Advancements in novel materials like bimetallic and trimetallic NPs with Au showed promising green route catalytic activities competing with enzymatic reaction and can overcome the difficulties of the ascribed method (like handling molds and free enzymes separation, wastewater removal and low space–time yield of biochemical plants etc.).[5,11,12,20] The obtained compositionally different trimetallic NPs were tested for the glucose oxidation ability. The change in pH in the reaction media because of formation of gluconic acid after oxidation primarily indicates the progress of oxidation. The pH values were dropped from ~9.5 (initial value) to ~5.31 and ~6.01 for LE and LE + CE mediated trimetallic NPs after 190 min of reaction time. The depletion of glucose during oxidation was directly measurable by the glucose strips with a visible color change and the glucose drop was found to be around ~30 mM/L and below from the initial 400 mM/L (Figure S5a, Supporting Information). The amount of gluconic acid was quantitatively estimated by a spectrophotometric method using aluminum sulfate. In this method the UV absorbance of gluconate increases linearly at 240 nm in the presence of Al^{3+} ion because of formation of the chelate. From the linear equation of the standard plot, unknown concentration of gluconic acid can be calculated. The samples from reactor bottles containing glucose in aqueous medium in the presence of LE and LE + CE mediated trimetallic NPs are exposed to 9.6 mM aluminum sulfate solution for UV–vis spectrometric analysis (Figure S5b, Supporting Information). The OD values after six times diluted reaction media at 240 nm are 1.125 ± 0.04 and 1.15 ± 0.05 for LE and LE + CE trimetallic NPs assisted solutions (Figure S5b, Supporting Information). Upon calculation, the average gluconic acid produced in media after 190 min was found to be 386.33 mM and 393.5 mM for the LE and LE + CE mediated NPs, respectively. The values indicate the glucose conversion percent was about 77% and 80% for respective two NPs. Noteworthy to mention that these values are superior than some reported studies within 190 min[5,12,20] In the catalytic reaction process, the as-prepared trimetallic NPs promote the oxidation process of aldehyde group of glucose into a carboxylic acid (gluconic acid) as per eq 1. Trimetallic NPs in our study

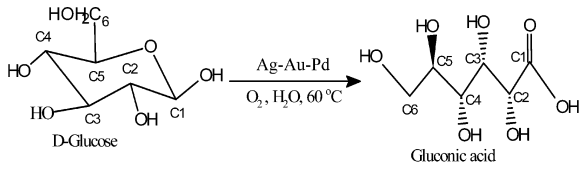

(1)

catalyzed the oxidation process of D-glucose to gluconic acid. The selective C_1-hydroxyl group oxidation of D-glucose in the presence of O_2 is the key step in the facile transformation.The catalytic activity was compared in terms of turnover frequency (TOF). The maximum TOF values obtained using two trimetallic NPs (LE and LE + CE) are 7333 and 7619 mol-glucose h^{-1}-mol-metal^{-1} respectively (Figure S5c, Supporting Information). The observed values are superior than the reported values by some monometallic Ag, Au, Cu, Pt, Pd, Rh NPs with TOF values ~110 to 4000 and bimetallic Au–Pt, Au–Ag, Au–Rh NPs with TOF values ~1000–5000.[5,12,20] The significant catalytic activity with low Pd content is noteworthy observation in our study and has the advantage of large scale production and application because of smaller size NPs in aqueous media through facile synthesis and greener approach for the first time.

Although the mechanism for the higher catalytic activity than the reported studies is still unclear, we believe that electronic charge transfer effect from the adjacent elements in the trimetallic NPs played a key role. Typically, the catalytic property enhancements by bi- and trimetallic NPs are mainly because of the electronic effect (ligand effect) and the geometrical effect (ensemble effect).[12] In ligand effect or ensemble effect, the mechanism for enhanced catalytic activity is attributed to higher electron density of the metal at the catalytic site by the addition of other metal atoms. The ligand effect is mostly applicable for core/shell type of multimetallic NPs, where the associated metal atoms are present adjacent to the catalytic metal atoms, but there is no direct contact with the reactant molecules and associated metal atoms. However, in geometrical effect, the reactant molecules have the chance to interact not only with the catalyst metal atoms but also with the associated metal atoms. Thus, both types of metal atoms can directly interact with the reactant molecules and affect the activity and selectivity of the reactants.[5,12] In our study, the geometrical effect is more important than the ligand effect.

DOI: 10.1021/acsami.5b03089
ACS Appl. Mater. Interfaces 2015, 7, 14018–14025

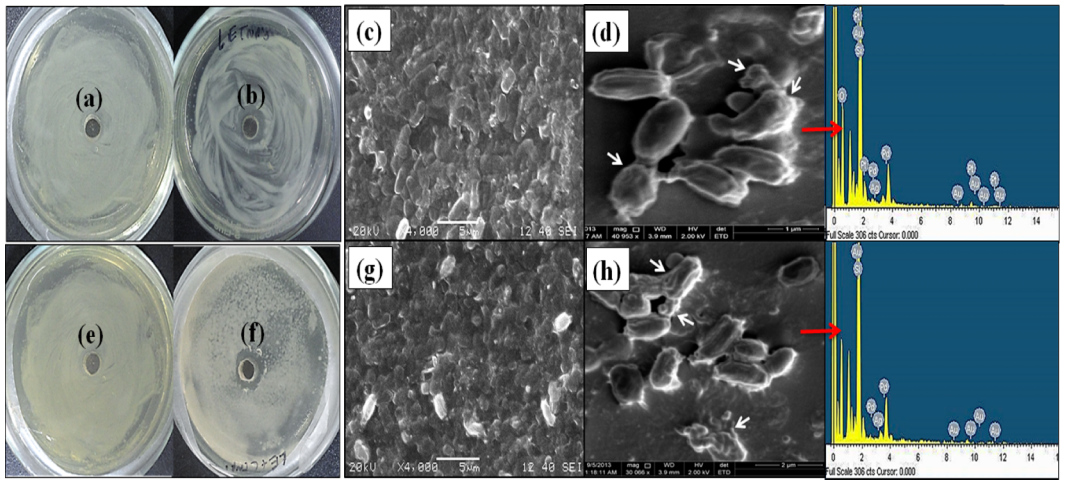

Figure 5. Inhibition zones of trimetallic NPs from LE (b) and LE + CE (f) against *E. coli* on nutrient agar plates. Twenty microliters of respective trimetallic NPs from 0.1 mM solution was given in each well, while control wells are with the respective plant extracts LE (a) and LE + CE (e) devoid of metal salts/NPs. The morphological changes of *E. coli* after exposure to 1 mL of 0.1 mM of trimetallic NPs from LE (c, d) and from LE + CE (g, h) is shown with the EDX analysis.

For instance, in the case of bimetallic NPs of Au−Ag, the enhancement of the catalytic activity is mainly because of one-way electronic charge transfer, from Ag to Au atom. However, for Au−Ag−Pd trimetallic NPs, the enhanced catalytic activity is attributed to the charge transfer between Ag → Au, Pd → Au, and sequential charge transfer from Ag → Pd → Au; which in turn increase the electron density on Au atoms. The high catalytic activity in alloy type trimetallic NPs (in particular Ag−Au−Pd) might be because of this synergistic effect of three types of charge transfer modes. This type of charge transfer may not be very active for core−shell type trimetallic NPs to show higher catalytic activity. Furthermore, monometallic NPs such as Au, Ag, and Pd also have catalytic action toward glucose oxidation but their activities are low.[5,12] In our case in addition to the electronic effect, the cumulative effect of all these metals also helps to enhance the catalytic activity. Apart from glucose oxidation, the synthesized Ag−Au−Pd NPs have huge scope to be utilized toward Heck, Sonogashira, and other chemical reactions.

3.6. Bacterial Sensitivity Tests. To evaluate the toxic effect of two types of trimetallic NPs produced; primarily agar plate studies were done with the bacterium *E. coli* (Figure 5a, b−e, f) with a constant dose NPs or controls in each agar well. The resultant ZOI values from Figure 5b and f are 0.99 and 0.96 mm for the NPs obtained from LE (∼8 nm) and LE + CE (∼11 nm) indicating no significant difference. Additionally, overnight grown *E. coli* cells are also exposed to 0.1 mM NPs of each type in aqueous media. Morphological evidence of SEM and FE-SEM analysis displayed vital alterations in the cell walls of *E. coli* treated with trimetallic NPs (Figure 5c, d−g, h) and the abrupt cell deformations indicated by arrows (white) in the figures. The presence of Ag/Au/Pd by EDX analysis of the bacterial cells of Figure 5d and h confirms the role of trimetallic NPs in structural deformation of *E. coli*.

Novel applications can be envisioned if we know the interactions between nanoscale materials and microorganisms. It is well-known that the antimicrobial behavior of metal NPs is governed by their size and composition. For instance, monometallic NPs like Au and Pd NPs dependent on size for effective antimicrobial activity,[29,30] but apart from size/shape, Ag NPs can adopt two or more mechanisms for the antimicrobial action.[31,32] In addition to the above, recent research also focused on assessments and utilization of antimicrobial properties of multimetallic NPs like bimetallic NPs eyeing on their multifunctionality[33,34] with no significant investigations on trimetallic NPs until to date. Our study showed that the as-prepared trimetallic NPs with Ag/Au/Pd are effective antimicrobial agents and with Au and Pd content, these were utilized for facile synthesis of gluconic acid which is industrially important biochemical transformation.

Along with biomedical applications, the synthesized NPs have huge scope to be multifunctional and can be used for improved electronic, optical and catalytic performances with Ag and Au content in it. Furthermore, with Pd content, it can be used as a novel catalyst in the chemical industry for carbon−carbon, carbon-heteroatom reactions and so on.

4. CONCLUSIONS

In this study, we have successfully synthesized novel Ag−Au−Pd NPs in a greener approach by employing plant extracts in a simplistic way for the first time. The methodology employed is capable of producing proportionally different Ag−Au−Pd NPs by simple tuning of the ratio of LE and CE. Uniform, reproducible trimetallic NPs of sizes ∼8 and ∼11 nm with smaller size distributions were produced instantaneously within few minutes. The trimetallic NPs thus prepared exhibited alloy type structures, which were confirmed by analyzing through HR-TEM, UV−visible, and XRD analysis. Along with the above analysis, the percentage crystallinity of the as-prepared trimetallic NPs with varying Pd proportions was also examined by XRD investigations. The use of mixed phytochemicals helps to vary the Pd % in the resultant NPs. Coming to glucose oxidation tests, the catalytic performance of the trimetallic NPs obtained from LE and LE + CE were tested under mild conditions without any external aeration or at high temperatures. More than 75% of conversion rate was achieved within 190 min by both trimetallic NPs used with reasonably good TOF values higher than Au containing bimetallic (Au−Pt, Au−Ag, Au−Rh) and other reported metallic (Ag, Au, Cu, Pt, Pd, Rh) particles. Furthermore, the antimicrobial potential of the synthesized Ag−Au−Pd NPs also showed significant toxicity toward the tested *E. coli* bacterium. Since gluconic acid is an

DOI: 10.1021/acsami.5b03089
ACS Appl. Mater. Interfaces 2015, 7, 14018−14025

important product for food and pharmaceutical industries, the developed catalyst with good catalytic and antimicrobial activities will be useful for higher yield as well as protect from the microbial contamination in the industrial process. The presence of Ag, Au, and Pd help these economically synthesized trimetallic NPs to be multifunctional and can be used as novel catalysts for widespread applications.

■ ASSOCIATED CONTENT

Supporting Information

Calculations of average molar mass and percentage crystallinity of trimetallic NPs, TEM images with different magnifications and size distribution of trimetallic NPs, calculated *d*-spacing values from SAED pattern, FESEM images and elemental mapping of trimetallic NPs synthesized from 0:1 proportion of LE + CE, glucose strip color changes, glucose depletion assay via aluminum salt solutions and TOF values of the used trimetallic NPs, IR analysis (in tabular form) of the plant systems used, and trimetallic NPs upon water wash. The Supporting Information is available free of charge on the ACS Publications website at DOI: 10.1021/acsami.5b03089.

■ AUTHOR INFORMATION

Corresponding Author

*E-mail address: santanuparia@yahoo.com or sparia@nitrkl.ac.in. Fax: +91 661 247 2926.

Notes

The authors declare no competing financial interest.

■ REFERENCES

(1) Toshima, N.; Yonezawa, T. Bimetallic Nanoparticles—Novel Materials for Chemical and Physical Applications. *New J. Chem.* **1998**, *22*, 1179−1201.
(2) Toshima, N. Capped Bimetallic and Trimetallic Nanoparticles for Catalysis and Information Technology. *Macromol. Symp.* **2008**, *270*, 27−39.
(3) Venkatesan, P.; Santhanalakshmi, J. Designed Synthesis of Au/Ag/Pd Trimetallic Nanoparticle-Based Catalysts for Sonogashira Coupling Reactions. *Langmuir* **2010**, *26*, 12225−12229.
(4) Zhan, G.; Huang, J.; Du, M.; Abdul-Rauf, I.; Ma, Y.; Li, Q. Green Synthesis of Au−Pd Bimetallic Nanoparticles: Single-Step Bioreduction Method with Plant Extract. *Mater. Lett.* **2011**, *65*, 2989−2991.
(5) Zhang, H.; Toshima, N. Preparation of Novel Au/Pt/Ag Trimetallic Nanoparticles and their High Catalytic Activity for Aerobic Glucose Oxidation. *Appl. Catal., A* **2011**, *400*, 9−13.
(6) Zhang, X.; Zhang, F.; Chan, K.-Y. Preparation of Pt−Ru−Co Trimetallic Nanoparticles and their Electrocatalytic Properties. *Catal. Commun.* **2004**, *5*, 749−753.
(7) Toshima, N.; Ito, R.; Matsushita, T.; Shiraishi, Y. Trimetallic Nanoparticles Having a Au-Core Structure. *Catal. Today* **2007**, *122*, 239−244.
(8) Tsai, S.-H.; Liu, Y.-H.; Wu, P.-L.; Yeh, C.-S. Preparation of Au−Ag−Pd Trimetallic Nanoparticles and Their Application as Catalysts. *J. Mater. Chem.* **2003**, *13*, 978−980.
(9) Karthikeyan, B.; Loganathan, B. Rapid Green Synthetic Protocol for Novel Trimetallic Nanoparticles. *J. Nanopart.* **2013**, *2013*, 1−8.
(10) Wang, L.; Yamauchi, Y. Strategic Synthesis of Trimetallic Au@Pd@Pt Core−Shell Nanoparticles from Poly(Vinylpyrrolidone)-Based Aqueous Solution toward Highly Active Electrocatalysts. *Chem. Mater.* **2011**, *23*, 2457−2465.
(11) Zhang, H.; Okumura, M.; Toshima, N. Stable Dispersions of PVP-Protected Au/Pt/Ag Trimetallic Nanoparticles as Highly Active Colloidal Catalysts for Aerobic Glucose Oxidation. *J. Phys. Chem. C* **2011**, *115*, 14883−14891.
(12) Zhang, H.; Toshima, N. Glucose Oxidation Using Au-Containing Bimetallic and Trimetallic Nanoparticles. *Catal. Sci. Technol.* **2013**, *3*, 268−278.
(13) Mohanpuria, P.; Rana, N. K.; Yadav, S. K. Biosynthesis of Nanoparticles: Technological Concepts and Future Applications. *J. Nanopart. Res.* **2007**, *10*, 507−517.
(14) Dahl, J. A.; Maddux, B. L. S.; Hutchison, J. E. Toward Greener Nanosynthesis. *Chem. Rev.* **2007**, *107*, 2228−2269.
(15) Govindaraju, K.; Basha, S.; Kumar, V.; Singaravelu, G. Silver, Gold and Bimetallic Nanoparticles Production Using Single Cell Protein (*Spirulina platensis*) Geitler. *J. Mater. Sci.* **2008**, *43*, 5115−5122.
(16) Tamuly, C.; Hazarika, M.; Borah, S. C.; Das, M. R.; Boruah, M. P. In Situ Biosynthesis of Ag, Au and Bimetallic Nanoparticles Using *Piper pedicellatum* C.DC: Green Chemistry Approach. *Colloids Surf., B* **2013**, *102*, 627−634.
(17) Karthikeyan, B.; Loganathan, B. Strategic Green Synthesis and Characterization of Au/Pt/Ag Trimetallic Nanocomposites. *Mater. Lett.* **2012**, *85*, 53−56.
(18) Loganathan, B.; Karthikeyan, B. Au Core Pd/Pt Shell in Trimetallic Au/Pd/Pt Colloidal Nanocomposites—Physicochemical Characterization Study. *Colloids Surf., A* **2013**, *436*, 944−952.
(19) Haverkamp, R. G.; Marshall, A. T.; van Agterveld, D. Pick Your Carats: Nanoparticles of Gold−Silver−Copper Alloy Produced in Vivo. *J. Nanopart. Res.* **2007**, *9*, 697−700.
(20) Comotti, M.; Pina, C. D.; Rossi, M. Mono- and Bimetallic Catalysts for Glucose Oxidation. *J. Mol. Catal. A: Chem.* **2006**, *251*, 89−92.
(21) Rao, K. J.; Paria, S. Green Synthesis of Silver Nanoparticles from Aqueous *Aegle marmelos* Leaf Extract. *Mater. Res. Bull.* **2013**, *48*, 628−634.
(22) Biswal, N. R.; Paria, S. Interfacial and Wetting Behavior of Natural−Synthetic Mixed Surfactant Systems. *RSC Adv.* **2014**, *4*, 9182−9188.
(23) Raghunandan, D.; Bedre, M. D.; Basavaraja, S.; Sawle, B.; Manjunath, S.; Venkataraman, A. Rapid Biosynthesis of Irregular Shaped Gold Nanoparticles from Macerated Aqueous Extracellular Dried Clove Buds (*Syzygium aromaticum*) Solution. *Colloids Surf., B* **2010**, *79*, 235−240.
(24) Rao, K. J.; Paria, S. *Aegle marmelos* Leaf Extract and Plant Surfactants Mediated Green Synthesis of Au and Ag Nanoparticles by Optimizing Process Parameters Using Taguchi Method. *ACS Sustainable Chem. Eng.* **2015**, *3*, 483−491.
(25) McIntyre, J. F.; Foley, R. T.; Brown, B. F. Ultraviolet Spectra of Aluminum Salt Solutions. *Inorg. Chem.* **1982**, *21*, 1167−1172.
(26) Smith, D. J. In *RSC Nanoscience & Nanotechnology*; Hutchison, J., Kirkland, A., Eds.; Royal Society of Chemistry: Cambridge, 2008; pp 1−27.
(27) Link, S.; Wang, Z. L.; El-Sayed, M. A. Alloy Formation of Gold−Silver Nanoparticles and the Dependence of the Plasmon Absorption on Their Composition. *J. Phys. Chem. B* **1999**, *103*, 3529−3533.
(28) Yang, X.; Li, Q.; Wang, H.; Huang, J.; Lin, L.; Wang, W.; Sun, D.; Su, Y.; Opiyo, J. B.; Hong, L.; Wang, Y.; He, N.; Jia, L. Green Synthesis of Palladium Nanoparticles Using Broth of *Cinnamomum camphora* Leaf. *J. Nanopart. Res.* **2009**, *12*, 1589−1598.
(29) Zhou, Y.; Kong, Y.; Kundu, S.; Cirillo, J. D.; Liang, H. Antibacterial Activities of Gold and Silver Nanoparticles Against *Escherichia coli* and *Bacillus calmette-Guérin*. *J. Nanobiotechnol.* **2012**, *10*, 19.
(30) Adams, C. P.; Walker, K. A.; Obare, S. O.; Docherty, K. M. Size-Dependent Antimicrobial Effects of Novel Palladium Nanoparticles. *PLoS One* **2014**, *9*, No. e85981.
(31) Darmanin, T.; Nativo, P.; Gilliland, D.; Ceccone, G.; Pascual, C.; De Berardis, B.; Guittard, F.; Rossi, F. Microwave-Assisted Synthesis of Silver Nanoprisms/Nanoplates Using a "Modified Polyol Process". *Colloids Surf., A* **2011**, *395*, 145−151.
(32) Chaloupka, K.; Malam, Y.; Seifalian, A. M. Nanosilver as a New Generation of Nanoproduct in Biomedical Applications. *Trends Biotechnol.* **2010**, *28*, 580−588.

DOI: 10.1021/acsami.5b03089
ACS Appl. Mater. Interfaces 2015, 7, 14018−14025

(33) Li, T.; Albee, B.; Alemayehu, M.; Diaz, R.; Ingham, L.; Kamal, S.; Rodriguez, M.; Bishnoi, S. W. Comparative Toxicity Study of Ag, Au, and Ag−Au Bimetallic Nanoparticles on *Daphnia magna*. *Anal. Bioanal. Chem.* **2010**, *398*, 689−700.
(34) Banerjee, M.; Sharma, S.; Chattopadhyay, A.; Ghosh, S. S. Enhanced Antibacterial Activity of Bimetallic Gold−Silver Core−Shell Nanoparticles at Low Silver Concentration. *Nanoscale* **2011**, *3*, 5120−5125.

DOI: 10.1021/acsami.5b03089
ACS Appl. Mater. Interfaces 2015, 7, 14018−14025